

Evaluation and utilization of MODIS and CALIPSO aerosol retrievals over a complex terrain in Himalaya

Ashish Kumar^{1,2}, Narendra Singh¹, Anshumali², Raman Solanki³

¹Aryabhatta Research Institute of Observational Sciences (ARIES), Manora peak, Nainital, India

²Indian Institute of Technology (Indian School of Mines), Dhanbad, India

³National Astronomical Research Institute of Thailand (NARIT), Chiangmai, Thailand

Abstract

10 The study elucidate upon the evaluation of satellite retrievals with ground based aerosol optical
11 depth (AOD) measurements, their utilization in LiDAR ratio (LR) estimation, boundary layer
12 (BL) height determination and the case studies on aerosol transport over Himalayan region. The
13 AOD retrievals from the latest level-2 data collections (C5.1 and C6.0) of MODerate resolution
14 Imaging Spectroradiometer (MODIS) onboard Aqua and Terra satellites and Cloud-Aerosol
15 LiDAR and Infrared Pathfinder Satellite Observations (CALIPSO) versions (4.10 and 3) are
16 subjected for quantitative analysis to assess the level of agreement with the quality assured level-
17 2 ground based AErosol RObotic NETwork (AERONET) measurements over Manora peak
18 (29.36° N, 79.46°E), a high altitude site in the Himalayas. Analysis revealed that the AOD from
19 the latest MODIS Terra C6.0 deep blue (DB) 30 km × 30 km and CALIPSO ver. 4.10 (overpass
20 within ~100 km distance) are in a very good agreement ($R \geq 0.9$) with that from coincident
21 AERONET measurements averaged over the span of ±30 minutes. About 77 % of the AOD
22 retrieved using MODIS and ~ 87 % from CALIPSO were found to be within the expected error
23 (EE) limits. The AOD comparison between MODIS Terra C6.0 DB and CALIPSO ver. 4.10,

24 suggested their synergic use for aerosol characterization over Himalayas. In comparison to the
25 ver. 3, CALIPSO ver. 4.10 is found to have undergone substantial changes, and their long term
26 inter-comparison in the grid 28.86°-29.86° N and 78.96°-79.96° E revealed that their vertical
27 feature and aerosol sub-types are in agreement of ~ 94.6 % and ~ 68.6 %, respectively. Utilizing
28 the AOD retrievals from AERONET and MODIS collections, the iteratively computed LR for
29 three LiDAR systems was found to be lower (< 16) during winter and higher (> 43) during
30 summer. Study on the BL height estimations suggested that the wavelet covariance transform
31 (WCT) method for CALIPSO could be the best choice as compared to the threshold method, and
32 complements well with the specific humidity gradient method used with the radiosonde
33 observation. Case studies on the continental transport of smoke plumes emanating from crop-
34 residue burning in post-monsoon, and long range transport of aerosols and dust over the region in
35 summer are also discussed using the collocated measurements from ground-based AERONET
36 and LiDAR, in conjunction with MODIS, CALIPSO, reanalysis data and trajectory modeling.

37

38 **Keywords:** Aerosols, CALIPSO, AOD, AERONET, MODIS, LiDAR, LR, radiosonde, dust,
39 smoke

40

41 **1. Introduction**

42 The phenomena such as fossil fuel combustion and biomass burning are directly linked to
43 the anthropogenic activities across the globe, affecting the weather and climate at various spatial
44 and temporal scales. These anthropogenic sources as well as the natural sources like air-borne
45 dust, storms etc. can alter the concentration, chemical composition, size distribution and shapes
46 of the atmospheric aerosols (Boucher, 2015). Any such alterations in aerosol distribution can
47 affect the climate on regional as well as on global scales (IPCC, 2014; Hansen and Sato, 2016).
48 The understanding of the atmospheric aerosol sources and their variations over a region in
49 conjunction with the prevailing meteorological conditions may improve the knowledge of
50 atmospheric processes such as the radiation balance, cloud formation, precipitation and chemical
51 processes aloft. Rising concerns on climate change demand better insight of the physical and
52 optical properties of the aerosols by means of ground and satellite based measurements such as
53 AERONET, LiDAR, CALIPSO and MODIS. The correlations and improved understanding on
54 the relationship between ground based and space borne observations are also essential in
55 formulating the reliable current and future predictions (Ramachandran and Kedia, 2013).
56 Moreover, it is important that any artefacts or inconsistencies associated with theoretical or
57 operational exactitudes in the aerosol measurements are to be checked and understood.

58 Past studies have emphasized that satellites are the best tool for broader understanding of
59 aerosol parameters on a global scale, however, satellite measurements possess some
60 uncertainties, especially, at the local scale which can be quantified through their assessment with
61 the ground based measurements (Kokhanovsky et al., 2007; Hersey et al., 2015). In this context,
62 it is important that the satellite based latest release of aerosol products are to be examined, from
63 time to time and corrected with the ground truth on a regional scale at finer spatial resolutions.

64 Nevertheless, while dealing with the aerosol optical product retrieval algorithms, it is quite
65 common to make some priori assumptions in the retrieval processes that sometime may lead to
66 the erroneous results and incorrect conclusions. One such assumption is the unknown aerosol LR
67 value of any Mie LiDAR system whose wrong selection may produce uncertainty in the
68 calculation of aerosol extinction coefficients and AOD values. Likewise, the aerosol retrieval
69 algorithms based on satellite data demand such assumptions regarding aerosol optical properties
70 e. g. single scattering albedo (SSA) and refractive index (Kokhanovsky et al., 2007; Wang et al.,
71 2011). Hence, the rigorous assessment of these products is essential for studies on aerosol
72 distribution.

73 Furthermore, the regional climate, particularly, along the slopes of the mountain regions,
74 is being greatly affected due to the deleterious anthropogenic interventions. The preliminary
75 assessment of climate change with impact studies on temperature and rainfall, snow cover and
76 glaciers, biodiversity, streams and rivers, agriculture and other sectors conducted by state of
77 Uttarakhand have been reported (Mishra, 2014; UCOST and USERC, 2012). However, there are
78 a very limited studies focusing on the long term impacts of aerosols on Himalayan ecosystem,
79 due to lack of high resolution ground based measurements (Mal et al., 2016). Studies focused on
80 Himalayan region are of paramount importance, as the occurrences of cloudbursts, flash floods,
81 landslides etc. have increased over the region due to the human's overexploitation of natural
82 resources by rapid urbanization, industrialization, deforestation, emissions from forest-fires,
83 transportation etc. (Valdiya, 2008; Tiwari and Joshi, 2016).

84 Considering the aforementioned facts, an attempt is made to evaluate the latest versions
85 of satellite aerosol products mainly AOD, at regional scale and compared/validated with the
86 ground truth as previously done by the researchers (e.g. Choudhry et al., 2012; Solanki and

87 Singh, 2014) on the earlier versions. This would enable subsequent usage of these products for
88 understanding the aerosol characteristics and their impact over the region. Focusing the
89 AERONET observations over the Himalayan region, LR for different LiDAR systems is
90 estimated and discussed using collocated measurements along with the MODIS satellite
91 retrievals. The latest CALIPSO aerosol products are also quantitatively evaluated with its earlier
92 versions and utilized in BL height determination over the complex terrain, as BL evolution is a
93 key parameter to understand the vertical transport of pollutants. Hence, making use of the
94 evaluated data sets, the transport mechanism of the aerosols from distant regions (continental and
95 long range) is studied and explained with the trajectory model, reanalysis data, and satellite
96 products. The subsequent sections describe about site, instrumentation and data, methodologies,
97 results and discussion, which is followed by the conclusion at the end.

98

99 **2. Site, instrumentation and data**

100 *2.1. Site Description*

101 Manora peak (29.36° N, 79.46°E, 1939 m amsl) is a high altitude regional representative
102 site in the central Himalayas located near the city of Nainital in the state of Uttarakhand (Solanki
103 and Singh, 2014; Solanki et al., 2016). The study using ground and satellite based measurements
104 over the site amidst undulating topography in the free tropospheric conditions can be of great
105 relevance. This pristine site is surrounded by the Himalayan mountain ranges and towards its
106 South is the Indo-Gangetic plains (known as Tarai). During the past two decades,
107 industrialization has grown up rapidly in these Tarai portions (Kazuo, 2014) and the pollutants
108 are being transported to the site quite often (Ojha et al., 2012; Sarangi et al., 2014). Therefore,
109 the site has a great advantage to study the continental as well as long range transport of the

110 pollutants, and additionally it provides the background values of the aerosol parameters. Further
111 details of the site, variations in meteorology and synoptic-wind patterns can be found elsewhere
112 (Ojha et al., 2014; Singh et al., 2016). The data sources used in the present study are described in
113 the subsequent sub-sections.

114 *2.2. LiDAR observations*

115 During the period from 2006 - 2014, three Mie LiDAR systems at Manora peak were
116 utilized for the vertical profiling of atmospheric aerosols in the free troposphere. The first system
117 was operated during 2006-2008 (Hegde et al., 2009), and the second system between 2010 and
118 the mid of 2011 (Bangia et al., 2011). The third system named as LiDAR for Atmospheric
119 Measurement and Probing (LAMP) is an upgraded version of the first one and was made
120 operational since October 2011 (Solanki et al., 2013; Solanki and Singh, 2014). LAMP is much
121 more compact monostatic version of the first one and is equipped with RS-232 and Ethernet
122 interfaces, built-in acousto-optic modulator for Q-switching and high quality optical assemblies.
123 **Table 1** summarizes the major differences among all the three versions of LiDAR systems. All
124 LiDAR systems at the study site were operated in late-evening hours under cloud free conditions
125 on the days considered in this study, and the data acquired is presented collectively.

126 **Table 1.**

127 Technical specifications of the Mie LiDAR systems operated at the site.

<i>Parameters</i>	LiDAR-I	LiDAR-II	LiDAR-III
Wavelength	532 nm	532 nm	532 nm
Telescope	Cassegrain, 150 mm dia, ~ 1 mrad Focal ratio – f/9	Cassegrain, 380 mm dia, ~ 6 mrad Focal ratio – f/15	Cassegrain, 150 mm dia, ~ 400 μ rad Focal ratio – f/9

Laser Type	Q-switched, Nd:YAG	Q-switched, Nd:YAG	Acousto-optic, Q-switched, Nd:YAG
Beam expander	8X	10X	8X
Resolution	30 m	300 m	15 m
Complete Overlap	150 m	300 m	90 m

128

129

130 *2.3. AERONET measurements*

131 The AERONET program is an inclusive federation of ground-based remote sensing
 132 aerosol networks established by National Aeronautics and Space Administration (NASA) and
 133 PHOtométrie pour le Traitement Opérationnel de Normalisation Satellitaire (PHOTONS) and
 134 greatly expanded by networks and collaborators from national agencies, institutes, and other
 135 partners (Holben et al., 1998). The program provides a long-term database of globally distributed
 136 observations of aerosol optical, microphysical and radiative properties. AERONET
 137 measurements are considered to be the ground truth due to its worldwide use and acceptability in
 138 the validation and bias corrections of the satellite retrievals (Bréon et al., 2011; Bibi et al., 2015;
 139 Bilal et al., 2016).

140 In the present study, the quality assured and well calibrated, level-2 AERONET data sets
 141 are used that include automatic cloud screening and utilize the tools such as 1-min stability,
 142 diurnal stability, smoothness tests etc. The day-time measurement of columnar aerosol
 143 parameters at wavelengths between 440 – 870 nm using the collocated AERONET sun
 144 photometer system, are utilized with the coincident night-time LiDAR observations. The
 145 AERONET provides the high quality data on a wider scale across the globe, so the
 146 methodologies adopted in the present work can be utilized by the larger science community.

147

148 2.4. *MODIS products*

149 MODIS is a key Earth observing instrument launched aboard NASA's Terra (MOD) and
150 Aqua (MYD) satellites on 18 December 1999 and 4 May 2002 respectively (Savtchenko et al.,
151 2004). Terra's orbit around the Earth is so timed that it passes from North to South across the
152 Equator (descending node) in the morning, while Aqua passes South to North over the Equator
153 (ascending node) in the afternoon. MODIS satellite passes over the study region twice a day and
154 specifically, Terra crosses between 10:00 – 11:00 hours local time (LT), while Aqua between
155 13:00 – 14:00 hours LT. MODIS Terra and Aqua satellites view the entire Earth's surface in
156 every 1 to 2 days, acquiring data since March 2000 for Terra, and July 2002 for Aqua in 36
157 spectral bands between 0.4 and 14.4 μm . The acquired MODIS data are available in the
158 hierarchy of levels (level-1 to 4) and grouped in four broad disciplines – land, atmosphere, ocean
159 and cryosphere. The collections are also defined in MODIS data that represent the versions of
160 MODIS data production algorithm (Savtchenko et al., 2004; Remer et al., 2005). In the present
161 work, level-2 MODIS aerosol collections (C5.1 and C6.0) and active fire location product (C6.0)
162 available under atmosphere and land disciplines respectively are used.

163 The latest level-2 MODIS aerosol product collections C5.1 and C6.0 over land and ocean
164 are based on two algorithms, namely the deep blue (DB) and dark target (DT) (Remer et al.,
165 2005; Levy et al., 2013; Bilal et al., 2016). DT has separate algorithms for land and ocean,
166 whereas DB is for the land retrieval only. Both C5.1 and C6.0 contains the standard 10 km
167 spatial resolution MODIS Terra (MOD04_L2) and Aqua (MYD04_L2) retrievals. To cater the
168 need of resolving the local aerosol gradients and regional features in a much precise manner, the
169 MODIS C6.0 production includes the DT aerosol product with 3 km spatial resolution under
170 both Terra (MOD04_3K) and Aqua (MYD04_3K) platforms. Recent studies revealed that the

171 MODIS 3 km land product is less reliable and requires continued evaluation in contrast to the
172 standard 10 km product (Remer et al., 2005; Levy et al., 2013; Remer et al., 2013; Nichol and
173 Bilal, 2016; He et al., 2017). Studies were carried out on the validation of MODIS 10 km aerosol
174 retrievals over land with the ground based measurements, and over ocean with the shipborne
175 measurements (Remer et al, 2002; Remer et al., 2005; Wang et al., 2011; Sayer et al., 2013).
176 Majority of the cited studies have found reliable and good agreements of the 10 km retrievals
177 with ground based measurements. Therefore, here 10 km MODIS level-2 latest C6.0 (DT and
178 DB) and C5.1 (DT) with quality flag 3 were chosen for assessment and comparison with the
179 ground truth over the region.

180 For one of the case studies presented in section 4, the MODIS C6.0 standard active fire
181 location product MCD14ML is extracted from NASA Fire Information for Resource
182 Management System (FIRMS) database which is produced using the most up-to-date algorithms
183 in the form of monthly files containing the geographic location, date, brightness temperature,
184 updated fire radiative power (FRP), fire type and the confidence levels for each fire pixel
185 detected by the Terra and Aqua MODIS sensors. The confidence estimate is expressed in
186 percentage and is classified as 0% - 29 % for low, 30% - 79% for nominal, and 80% - 100% for
187 high fire-events (Giglio et al., 2003; Giglio, 2005).

188 *2.5. CALIPSO products*

189 CALIPSO was launched in April 2006 under a joint mission of NASA and the French
190 space agency, Centre National d'Etudes Spatiales (CNES). It is equipped with a dual wavelength
191 (550 and 1064 nm) polarization LiDAR system referred as Cloud and Aerosol LiDAR with
192 Orthogonal Polarization (CALIOP) for providing the long term database of global aerosol
193 vertical profiles (Winker et al., 2009 and 2010). The CALIOP laser transmitter is a diode-

194 pumped Nd:YAG laser that emits simultaneous co-aligned pulses at 532 and 1064 nm. The laser
195 generates optical pulses of ~20 ns long with 110 mJ of energy at both the wavelengths. The
196 receiver sub-systems measures the backscattered signal intensity at 1064 nm and the two
197 backscattered orthogonal polarization components at 532 nm (Winker et al., 2009 and 2010;
198 Hunt et al., 2009).

199 At present, the researchers worldwide, are utilizing the CALIPSO products to a great
200 extent in order to understand the impact of aerosol and cloud on the Earth's radiation budget.
201 The CALIPSO/CALIOP (*ver. 3 and 4.10*) aerosol products used in this study are:

- 202 ▪ *Level-1B* products (temporal resolution: 0.05 sec, vertical and spatial resolution: 30 m (0-
203 8.2 km) and 333 m)
- 204 ▪ *Level-2* products:
- 205 - Aerosol profile (temporal resolution: 5.92 sec, vertical and spatial resolution: 60 m × 5 km)
- 206 - Aerosol layer (temporal resolution: 0.74 sec, spatial resolution: 5 km)
- 207 - Vertical feature mask (VFM) product (temporal resolution: 0.74 sec, vertical and spatial
208 resolution: 30 m (up to 8.2 km) and 333 m)

209 *2.6. Reanalysis products*

210 The reanalysis products are produced from the available atmospheric observations and
211 dynamic models. There are a number of reanalysis products available on the global scale such as
212 NCEP-NCAR reanalysis (NNR), ERA-40, ERA-Interim, Modern-Era Retrospective analysis for
213 Research and Applications (MERRA) etc. (Decker et al., 2012). In the present study, to ascertain
214 the sources of dust transport, data obtained from MERRA-2 (ver. 5.12.4) is utilized. It is the
215 latest available reanalysis product released by NASA Global Modeling and Assimilation Office
216 (GMAO), and is based on the Earth observing system (EOS) satellite observations (Bosilovich et

217 al., 2016). The 6-hourly ERA-Interim wind products is also used to understand the prevailing
218 wind pattern over the site during the period of study.

219 *2.7. Air mass trajectory model*

220 To trace the sources of air masses on the days showing high AOD variabilities over the
221 site, the backward trajectory analysis is carried out using National Oceanic and Atmospheric
222 Administration (NOAA) Hybrid Single Particle Lagrangian Integrated Trajectory (HYSPLIT)
223 model (Draxler and Hess, 1997, 1998). The model utilizes several meteorological parameters
224 like rainfall, humidity, temperature and solar radiation flux for computing the air mass
225 trajectories at different height levels. The trajectory analysis basically characterizes the air
226 masses and the origin, in order to understand the impact on meteorological conditions and the
227 aerosol transport (Draxler and Hess, 1997, 1998; Stein et al., 2015).

228

229 **3. Methodology**

230 *3.1. Selection criteria for evaluation of satellite products*

231 Along with the intermittent observations made using LiDAR systems, the collocated
232 AERONET measurements were also available for the period of 2008- 2012. The AERONET
233 observation were made from the site in two phases – each during April 2008-February 2011
234 (Nainital Station) and August 2011-March 2012 (ARM_Nainital Station). Out of the datasets
235 collected during above period, common days of reliable measurements with best temporal match
236 were selected. Based on the LiDAR profiles the selected data were further screened for clear sky
237 conditions. In this process the usable datasets turned out to be 37, and considered for the
238 analysis.

239 In order to match with the above identified 37 days, the selection of MODIS data sets is
240 done on the basis of closest overpass to the site and the availability of AERONET data during
241 the overpass. The details on the number of spatially and temporally coincident data sets (N)
242 obtained as a result are given in **Table 2**. To achieve a valid comparison between AOD values
243 measured from MODIS and AERONET instruments, a well-known spatio-temporal averaging
244 technique is adopted (Ichoku et al., 2002) and multiple metrics were utilized to quantify the
245 results. Taking into account the mean MODIS AOD values within $20\text{ km} \times 20\text{ km}$ and $30\text{ km} \times$
246 30 km grid and AERONET AOD averaged over ± 30 minutes and ± 15 minutes, various cases on
247 spatio-temporal combinations were examined and the levels of agreement were established.

248 MODIS being the passive remote sensor provides a single columnar value of aerosol
249 parameter, which lacks the information of aerosol vertical distribution, a rather important
250 parameter to quantify aerosol effects in the atmosphere. In this context, the CALIPSO satellite
251 products were also evaluated and used in the BL height estimation and case studies on the
252 evolution and transport of aerosols. In order to understand the associated changes (vertical
253 features and aerosol sub-types) in the two versions (ver. 3 and 4.10) of CALIPSO data over
254 complex Himalayan terrain, level-2 VFM profiles available within the grid of $\pm 0.5^\circ$ ranging
255 from 28.86° - 29.86° N and 78.96° - 79.96° E for the period August 2006- April 2017 were
256 analysed. The results in the form of confusion matrix are presented and discussed in relevance to
257 the changes in the feature types and aerosol sub-types between ver. 3 and ver. 4.10 data. Further,
258 to evaluate the AOD values from two versions of CALIPSO with AERONET, a total of 23 data
259 sets were identified based on the criteria of high cloud aerosol discrimination (CAD) score
260 (between -35 and -100), the presence of 5 or more valid vertical profiles up to 4.5 km altitudes

261 within the horizontal distance of ~ 100 km from the site, and the availability of coincident
262 AERONET measurements within ± 30 minutes of the closest CALIPSO ground track.

263 For the period October 2006 – December 2014, 54 good cases of AOD measurements
264 both from the MODIS Terra DB C6.0 and CALIPSO (within 100 km) were identified, and the
265 same were utilized in their inter-comparison. The selection procedure is based on the screening
266 and coincidence constraints, and the sequence is as follows:

- 267 • To account for the best temporal match between the CALIPSO and MODIS satellite
268 overpasses, only the day-time CALIPSO profiles were considered where the time
269 difference between two observations is within 3 hours.
- 270 • For MODIS, the averaged AOD values (550 nm) with quality flag 3, measured within 30
271 $\text{km} \times 30 \text{ km}$ from the site were considered.
- 272 • For CALIPSO, the average of the column AOD values (532 nm) reported in CALIPSO
273 level-2 aerosol layer product is used. The selection criteria set for the AOD is: CAD score
274 (between -35 to -100), Extinction QC 532 flag (0 or 1), column optical depth uncertainty
275 (between 0 and $0.5 \times \text{AOD}$), CALIOP initial LR = final LR, surface elevation > 1200 m,
276 and the horizontal averaging ≤ 80 km (Young and Vaughan, 2009; Vaughan et al., 2016).

277

278 3.2. *LR estimations*

279 The LR for any single wavelength ground-based LiDAR is a key parameter that needs to
280 be known for the retrieval of aerosol vertical profiles. Basically, it is the ratio of aerosol
281 extinction coefficient (α_{aer}) and the aerosol backscatter coefficient (β_{aer}) that is linked to the
282 regional aerosol characteristics like shape, size and composition. A-priori hypotheses for LR in
283 the range between 20 to 100 sr is quite common, but LR computed by constraining the AOD

284 from LiDAR through AERONET or MODIS measurements can be the better choice than former
285 (He et al., 2006). In the later approach, initially the LiDAR range-corrected signal (RCS) is
286 processed for AOD computation with a fixed LR, which then undergoes several iterations to
287 produce an adjusted LR at a point where the difference between LiDAR derived AOD (τ_{LiDAR})
288 and the AOD retrieved from AERONET ($\tau_{AERONET}$) or MODIS (τ_{MODIS}) measurements is
289 minimal. Similar approach is adopted here to find out the best LR values for the three LiDAR
290 systems operated in night-time under clear-sky conditions during different seasons. The adjusted
291 range-independent LR values, where the LiDAR AOD showed the best match within the
292 tolerance of $\pm 0.5\%$, are considered to be the final LR. To account for any discrepancies between
293 day and night-time AOD measurements from AERONET and the ground based LiDAR, about
294 95% of the data sets were so chosen that the diurnal variations in AOD and AE (440-870 nm) fall
295 in the limits of ± 0.05 and ± 0.2 , respectively (Amiridis et al., 2011). Such a bound is employed to
296 ensure that the intrusion of aerosol from other locations is almost insignificant and the aerosol
297 loading remains nearly the same during day and night over the site.

298 The LiDAR AOD in LR retrieval process has been computed using the relation:

$$299 \quad \tau_{LiDAR,532} = \int_{z_0}^{z_1} \alpha_{aer}(z) dz + \int_{z_1}^{z_2} \alpha_{aer}(z) dz \quad (1)$$

300

301 where, z_0 = height at which the LiDAR system is installed, z_1 = height at which complete
302 overlap occurs (150 m, 300 m and 90 m considered for the three LiDAR systems, respectively),
303 and z_2 = upper height limit considered for the columnar AOD retrievals (assumed as 4.5 km
304 above ground level). Considering the uniform distribution of aerosols between z_0 to z_1 , it is
305 assumed that for the three LiDAR systems, the maximum of 7.5 %, 15 % and 5 % of the AOD
306 values, respectively are confined within the respective overlap regions.

307 *3.3. BL height estimation*

308 The BL height is an important meteorological parameter that determines the extent to
309 which the dispersion of pollutants, heat and moisture take place, and is very useful parameter for
310 weather, climate and pollution studies (Monks et al., 2009). In this context, an accurate
311 determination of BL height, using different data sources over the complex high altitude site,
312 where the upslope and downslope airflows vary with time, is of great interest. From Manora
313 peak site, the radiosonde launches were conducted four times a day during 2011-2012 (Singh et
314 al., 2016), so taking this an advantage, and considering the fact that BL depth can be derived
315 from the radiosonde (Seibert et al., 2000; Singh et al., 2016) and CALIPSO data (Jordan et al.,
316 2010; McGrath Spangler and Denning, 2012), an attempt is made to estimate and compare the
317 BL height computed from the in-situ radiosonde observations and near coterminous CALIPSO
318 level-1B data (< 100 km overpass distance; ver. 4.10). To ascertain cloud-free cases, the
319 parameters (signal intensity at the surface, depolarization ratio, color ratio and vertical features)
320 from CALIPSO level-1B and 2 data products are examined for the period June 2011- March
321 2012. After discarding the cloud contaminated profiles, a total of 10 day-time cloud-free
322 CALIPSO profiles, in the temporal match (< 2 hours) with the radiosonde observations were
323 identified and selected for BL height estimation. The day-time cases were selected to avoid the
324 influence of the residual layer and heavy surface inversion (Su et al., 2017).

325 To estimate the BL heights from radiosonde, the vertical gradient method is used for the
326 potential temperature (PT) and specific humidity (SH), that is expressed as:

$$327 \frac{dX(y_i)}{dy} = \frac{X(y_{i+1}) - X(y_i)}{y_{i+1} - y_i} \quad (2)$$

328 Here, $X(y_k)$ is used to represent the PT or SH values at altitude y_k , where k represents the height
329 intervals i up to 3.2 km amsl in vertical, that is selected on the basis of the characteristics studied

330 over Manora peak (Singh et al., 2016). The BL height is identified as the location of the
331 maximum vertical gradient for PT and SH changes (Seibert et al., 2000; Seidel et al., 2010).

332 To retrieve the BL height from CALIPSO, two methods, namely the threshold (Melfi et
333 al., 1985; Johnson et al., 2010) and WCT (Brooks, 2003; Compton et al., 2013), are used. With
334 the threshold method, the BL height is determined by finding the steepest gradient in total
335 aerosol backscatter coefficient profiles (CALIPSO level-1B). In WCT method, the Haar wavelet
336 function is applied to the total aerosol backscatter coefficient profile, and its first maxima where
337 the sharpest decrease in the total aerosol backscatter coefficient occurs is taken up as the BL
338 height (Baars et al., 2008). The implementation of WCT method is described using two
339 equations (Gamage and Hagelberg, 1993; Brooks, 2003):

340
$$W_f(a, b) = \frac{1}{a} \int_{z_b}^{z_t} \beta'_{total,532}(z) \psi\left(\frac{z-b}{a}\right) dz \quad (3)$$

341 and,
$$\psi\left(\frac{z-b}{a}\right) = \begin{cases} +1 & b - \frac{a}{2} \leq z < b \\ -1 & b \leq z \leq b + \frac{a}{2} \\ 0 & elsewhere \end{cases} \quad (4)$$

342

343 where, a = dilation parameter (scale); b = vertical translation i.e. altitude at which the
344 wavelet function is centered; $\beta'_{total,532}(z)$ = CALIPSO level-1B total aerosol backscatter
345 coefficients as the function of altitude; $W_f(a, b)$ = wavelet covariance transform as a function of
346 scale and translation; $\psi\left(\frac{z-b}{a}\right)$ is the Haar wavelet function, described as a symmetrical square
347 wave with positive and negative going amplitudes; z_t and z_b are the top and bottom altitudes of
348 $\beta'_{total,532}(z)$.

349 For retrieval of BL height with high degree of accuracy using the WCT method, it is
350 essential that the dilation, ‘ a ’ should be carefully chosen (Brooks, 2003). At small dilation value,
351 due to the spurious gradients and noisy $W_f(a, b)$ profile, it becomes very difficult to estimate the

352 correct BL height, and at extremely high dilation value, the BL height becomes too high or
 353 sometime may even get missed. Therefore, the BL height estimated from the mean profile of
 354 wavelet covariance transform, $\langle W_f(b) \rangle$, generated across the mid-range of dilation values, is
 355 considered as the optimum BL height in the present work, which is expressed as:

$$356 \quad \langle W_f(b) \rangle = \frac{1}{n} \sum_{i=1}^n W_f(a_i, b) \quad (5)$$

357 and the final BL height = $\max \langle W_f(b) \rangle$, for $z_b < b < z_t$. This approach of selecting and
 358 averaging multiple wavelet dilation values will reduce the bias in the final BL height estimation.
 359 An example demonstrating the sensitivity analysis and the selection of appropriate dilation range
 360 for a typical CALIPSO level-1B (ver. 4.10) total aerosol backscatter coefficients profile of 16
 361 June 2011 is available in the Supplementary data (**Figure S1 (a-d)**).

363 *3.4. Retrieval error and wavelength conversions*

364 The EEs associated with AERONET measured AOD (τ) and the corresponding MODIS
 365 retrievals are $\text{EE}_{\text{AERONET}} = \pm 0.01$ to ± 0.02 and $\text{EE}_{\text{MODIS}} = \pm (0.05+0.15\tau)$, respectively (Holben et
 366 al., 1998; Eck et al., 1999; Remer et al., 2005). Similarly, the EE associated with CALIPSO
 367 measurement is $\text{EE}_{\text{CALIPSO}} = \pm (0.05+0.4\tau)$ (Winker et al., 2009). The uncertainties in the
 368 AERONET measurements are wavelength (λ) dependent and are generally higher in the ultra
 369 violet spectral ranges.

370 MODIS and AERONET measure AOD at two different wavelengths 550 and 500 nm
 371 respectively, and to make a valid comparison between the two, AOD at 500 nm is converted to
 372 AOD at 550 nm by taking into account the Angstrom exponent (AE) provided by AERONET in
 373 the wavelength range of 440 - 870 nm, using the relation as follows (Eck et al., 1999):

$$374 \quad \tau_{\text{required}} = \tau_{\text{measured}} \left[\frac{\lambda_{\text{required}}}{\lambda_{\text{measured}}} \right]^{-\text{AE}} \quad (6)$$

375

376 where, $AE = -\frac{\log\left[\frac{\tau_{\lambda_1}}{\tau_{\lambda_2}}\right]}{\log\left[\frac{\lambda_1}{\lambda_2}\right]}$, τ_{λ_1} and τ_{λ_2} are the AOD values at wavelengths λ_1 and λ_2 .

377 Similar analogy is used to make the comparison of CALIPSO (532 nm) with AERONET. In all
378 the wavelength conversions, it is assumed that the errors introduced were negligible.

379 *3.5. Performance parameters*

380 To evaluate the performance of the aerosol retrievals from MODIS and
381 CALIPSO/CALIOP satellite products, the following statistical parameters were computed on N
382 coincident data sets:

383 (i) Mean bias error (MBE) = $\frac{\sum(\tau_{\text{Satellite}} - \tau_{\text{AERONET}})}{N}$, is the measure of overall bias error and the
384 values > 0 indicate overestimation, whereas the values < 0 represent underestimation of
385 the satellite retrieved AODs with the ground truth.

386 (ii) Average error ratio (AER) = $\frac{\sum(\tau_{\text{MODIS}} - \tau_{\text{AERONET}})}{N} \times \frac{1}{EE}$, is the measure of the comparison
387 between the actual error and the EE. $|AER| \leq 1$ is the good match, and $|AER| > 1$ represents
388 the poor match. In case of satellite data, $AER < 0$ represents underestimation of the
389 measurement, and $AER > 0$ reveals overestimation.

390 (iii) Root mean square error (RootMSE) – It is the root mean square of the error in the
391 regression, computed as the square root of the reduced Chi-square i.e. $\sqrt{\text{Reduced } \chi^2}$. It
392 provides the variability/standard deviations of the data from the regression line. Lower the
393 value of RootMSE, better will be the agreement between the regression and the data.

394 (iv) Percentage mean relative deviation (MRD) = $\frac{100}{N} \sum_{i=1}^N \frac{|M_{\text{version2}} - M_{\text{version1}}|}{M_{\text{version2}}}$, is the measure
395 of mean divergence of the data version 2 (M_{version2}) from the version 1 (M_{version1}).

396 (v) Percentage EE (%EE) = Percentage of AOD values falling within EE limits that is defined
397 in section 3.4. If out of N AOD values, M values falls within the EE limits, then, % EE =

398
$$\frac{M}{N} \times 100.$$

399 (vi) Standard deviation (SD) – It is a measure of how spread out a data set is, and is equal to the
400 square root of the variance. Mathematically, for N samples (X_1, X_2, \dots, X_N), SD =

401
$$\sqrt{\frac{\sum_{i=1}^N (X_i - \bar{X})^2}{N-1}}$$
, where, \bar{X} is the mean value of N samples.

402 (vii) Standard error of mean (SEM) = $\frac{SD}{\sqrt{N}}$, and is the measure of the variability associated with
403 estimating a mean.

404

405 **4. Results and discussion**

406 *4.1. Evaluation of Satellite aerosol retrievals – MODIS and CALIPSO*

407 *4.1.1. Assessment of MODIS collections with coincident AERONET measurements*

408 In order to make an assessment of MODIS collections (C5.1 and C6.0), four cases on
409 spatial and temporal comparisons were considered. In the first two cases, the average of MODIS
410 AOD within $20 \text{ km} \times 20 \text{ km}$ from the study site are compared with the average AOD from
411 AERONET within (a) ± 30 minutes and (b) ± 15 minutes, and in the latter two cases, the average
412 of MODIS AOD within $30 \text{ km} \times 30 \text{ km}$ are compared with the average AOD from AERONET
413 within (c) ± 30 minutes and (d) ± 15 minutes of the closest Terra/Aqua overpass occurrences.

414 From the statistics on the four spatio-temporal combinations, as given in **Table 2**, case (c) is
415 found to perform better with almost all the metrics in good agreement as compared to other three
416 cases. Since, MODIS Terra shows high correlation ($R \sim 0.90$) and high %EE (~ 62) in comparison
417 to Aqua ($R \sim 0.75$, %EE ~ 54) with ground based AERONET measurements. Therefore, one has

418 to essentially decide upon the most suitable collection of Terra retrievals out of C5.1 DT, C6.0
 419 DT and C6.0 DB.

420

421 **Table 2.**

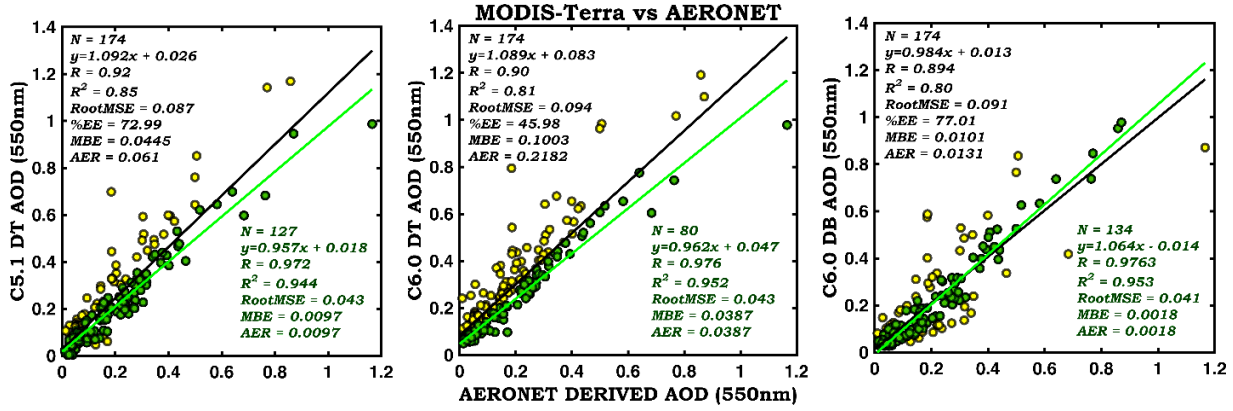
422 Statistical summary on AOD (550 nm) comparison for the four spatio-temporal cases.

		Case-(a)	Case-(b)	Case-(c)	Case-(d)
MODIS Terra DT: C5.1, C6.0 DB: C6.0	N	24	24	27	27
	Pearson Correlation (mean \pm SD \pm SEM)	0.90 \pm 0.05 \pm 0.03	0.89 \pm 0.05 \pm 0.03	0.90 \pm 0.04 \pm 0.02	0.90 \pm 0.03 \pm 0.02
	RootMSE (mean \pm SD)	0.068 \pm 0.02	0.069 \pm 0.02	0.067 \pm 0.01	0.068 \pm 0.02
	%EE (mean \pm SD)	52.8 \pm 17.4	48.6 \pm 17.3	61.7 \pm 15.5	56.8 \pm 17.1
	MBE (mean \pm SD)	0.052 \pm 0.04	0.052 \pm 0.04	0.054 \pm 0.04	0.054 \pm 0.04
	AER (mean \pm SD)	0.13 \pm 0.14	0.14 \pm 0.16	0.105 \pm 0.10	0.12 \pm 0.13
MODIS Aqua DT: C5.1, C6.0 DB: C6.0	N	22	21	22	22
	Pearson Correlation (mean \pm SD \pm SEM)	0.72 \pm 0.06 \pm 0.03	0.66 \pm 0.02 \pm 0.01	0.75 \pm 0.06 \pm 0.04	0.69 \pm 0.04 \pm 0.02
	RootMSE (mean \pm SD)	0.081 \pm 0.003	0.089 \pm 0.003	0.084 \pm 0.006	0.093 \pm 0.004
	%EE (mean \pm SD)	57.5 \pm 2.6	53.9 \pm 14.6	54.5 \pm 9.1	51.5 \pm 13.8
	MBE (mean \pm SD)	0.057 \pm 0.03	0.056 \pm 0.03	0.059 \pm 0.03	0.055 \pm 0.03
	AER (mean \pm SD)	0.102 \pm 0.06	0.12 \pm 0.10	0.12 \pm 0.08	0.13 \pm 0.11

423

424 In order to achieve the reasonable assessment with the ground truth, the study in case (c)
 425 is extended for 174 coincident AOD measurements available during 2008-2010. Each of the
 426 three collections is subjected to one-one line comparison with AERONET AOD values as shown
 427 in **Fig. 1**. From the figure, it is evident that MODIS Terra C5.1 DT showed high correlation (R
 428 \sim 0.92) and low RootMSE (\sim 0.087), thereby reflecting lowest variability, whereas, MODIS Terra
 429 C6.0 DB demonstrated the highest percentage of MODIS AOD values falling within the defined
 430 EE (\pm 0.05 \pm 0.15 τ) boundary (%EE \sim 77.01). However, MODIS Terra C6.0 DT is showing good
 431 correlation (R \sim 0.90), but the least %EE (\sim 45.98) among all.

432



433

434 **Fig.1.** Scatter plot with one-one line comparison for MODIS Terra and AERONET AOD
435 measurements; green + yellow = complete, green = for values within %EE.

436

437 Based on the %EE values, a total of 127, 80 and 134 data points respectively for C5.1
438 DT, C6.0 DT and C6.0 DB are found to be within EE limits, which are further subjected to
439 statistical analysis. The statistics confirms that the MODIS Terra C6.0 DB is the best choice
440 among others.

441 MBE and AER values for the three collections are found to be positive, indicating the
442 overestimation of MODIS AOD as compared to the ground based AERONET measurement. The
443 overestimation may be attributed to the huge spatial differences in measurements, as the ground-
444 based AOD measurement through AERONET is a point observation, whereas the MODIS
445 retrievals of AODs are over 10 km x 10 km at each instance. Owing to the large spatial coverage,
446 the MODIS retrieved AOD may get influenced due to the presence of small clouds, geographical
447 locations etc.

448 *4.1.2. Inter-comparison of CALIPSO versions*

449 CALIPSO mission announced the release of ver. 4.10 data product on 8 November 2016
450 and, in comparison to the earlier ver. 3, the quality in ver. 4.10 release is enhanced with the

451 inclusion of the updated digital elevation map (DEM) from CloudSat and high-quality MERRA-
452 2 product (Vaughan et al., 2016).

453 In going from CALIPSO ver. 3 to ver. 4.10, major code and algorithm modifications
454 were implemented, e.g. improved data filtering strategies, changes in the calibration algorithms
455 for both 532 nm and 1064 nm, and the revised probability density functions (PDFs) in CAD
456 algorithm. To investigate the changes in the vertical features provided by two CALIPSO
457 versions, an analysis is performed by extracting the feature classification flag (FCF) of each
458 detected layer from the VFM files for the CALIPSO transacts within the defined geographical
459 region of 28.86°-29.86° N and 78.96°-79.96° E for the period of August 2006- April 2017. The
460 vertical feature type, with a confidence level of at least ‘medium’ i.e. $50 \leq |\text{CAD score}| < 70$ for
461 aerosol and cloud layers (confirmed using FCF bits 4 and 5), is obtained by decoding the FCF
462 bits 1-3 in decimal form (Vaughan et al., 2016). The changes w.r.t. ver. 3, as observed in ver.
463 4.10 are explained by constructing a confusion matrix as given in the **Table 3**. The overall
464 agreement between ver. 3 and ver. 4.10 in this case is computed by summing the samples which
465 remained unchanged (e.g. clear air – clear air, cloud - cloud) divided by the total number of
466 samples expressed in percentage, and is found to be 94.64 % when a total of 437 day and night-
467 time profiles were taken into account. The level of disagreement between ver. 3 and ver. 4.10 is
468 ~1 % higher in the night-time profiles as compared to the day-time profiles (refer Supplementary
469 data **Table S1 and S2**).

470

471

472

473